ELSEVIER

Journal of Molecular Catalysis A: Chemical 144 (1999) 329–335

JOURNAL OF MOLECULAR CATALYSIS A: CHEMICAL

www.elsevier.com/locate/molcata

# Synthesis of NiAPSO-34 catalysts containing a larger concentration of Ni and effect of its sulfidation on methanol conversion

Misook Kang, Tomoyuki Inui *,1

*Department of Energy and Hydrocarbon Chemistry, Graduate School of Engineering, Kyoto University, Sakyo-Ku, Kyoto 606-01, Japan*

Received 30 April 1998; accepted 13 October 1998

**Abstract**

In order to obtain the NiAPSO-34 crystal containing a larger concentration of nickel, the nickel formate was used as the nickel source. It was confirmed that not only the amount of incorporated nickel into the framework but also the amount of the non-incorporated nickel increased, and in consequence, it involved methanation activity. To retard the methanation activity, sulfidation of the Ni non-incorporated was tried. In the case of $H_2S$ addition, methane formation suppressed markedly and selectivity to ethylene increased. 

*Keywords:* NiAPSO-34; Nickel formate; Nickel non-incorporated; Sulfidation

## 1. Introduction

Alternative routes of effective ethylene synthesis are now gaining increasing importance. After the innovation in synthesis of aluminophosphate molecular sieves by UCC [1,2], a trial of methanol conversion had been done using SAPO-34 as the catalyst for methanol conversion [3–6]. However, CHA has large cavities inside the crystal channel structure, which involves a risk of rapid coke formation as chabazite catalysts have [7], when the strength and number of acid sites inside the cavity are too much. The incorporation of Ni into the framework of SAPO-34 structure weakened the acid strength properly for methanol-to-ethylene conversion [4]. However, in our previous paper [8], it was suggested that the non-incorporated nickel exhibits the activities for methanol decomposition to hydrogen and carbon monoxide and consequently methanation resulting in the decrease in ethylene selectivity. In order to retard the activities of the non-incorporated nickel, the effect of the kind of nickel source to be mixed into the gel as the precursor was investigated [9]. As a result, it was clarified that the nickel sources have influence on the shape and

* Corresponding author. Tel: +81-774-32-9017; Fax: +81-774-32-2368

[1] Present address (Home): 5-43, 1-Chome, Hatoyama, Uji 611-0012, Japan.

1381-1169/99/$ - see front matter 
PII: S1381-1169(98)00362-8

physical properties of NiAPSO-34 crystals. In particular, small size crystals containing a larger concentration of Ni converted methanol selectively to ethylene. However, the control of non-incorporated nickel in cavity could not be perfectly resolved. On this point, Kang and Inui [10] suggested that the sulfidation on NiAPSO-34 crystal was useful to control the activity of the non-incorporated nickel in cavity.

On the other hand, $SO_2$ or $H_2S$ adsorption on the surface of metal oxides, such as MgO, CaO, and $Al_2O_3$ [11–15] and $H_2S$ adsorption on Na-zeolites [16–20] has been studied, and the predominant effects of $H_2S$ adsorption on zeolites, metal oxides or heteropoly acids upon hydrocarbon conversion [21] and hydrosulfurization of alcohols [22] have been observed. In these papers, it has been confirmed that the proper sulfidation has a strong influence on the acidity and activity of the catalyst.

Therefore, in the present study, $SO_2$ or $H_2S$ is added to methanol conversion expecting the inhibition of the activities for the decomposition of methanol and methanation by sulfiding the non-incorporated nickel.

## 2. Experimental

### 2.1. Catalyst

The catalyst was prepared by applying the rapid crystallization method [3,23] to the procedure for the synthesis of NiAPSO-34 described in the patent literature [1]. The detailed procedure for the preparation of reactive hydrogels of catalyst is described as follows; a 61.28 g of aluminum isopropoxide and $x$ g of each nickel source (nickel nitrate or formate) were added to 126.22 g of tetraethylammonium hydroxide in a 500 ml beaker and then stirred vigorously for 5 min with the homogenizer, and then a 9.01 g portion of Cataloid 30 (Shokubai Kasei; Content of $SiO_2$ 30 wt.%), 34.59 g of phosphoric acid (Wako Tech.; 85 wt.%) and 30 ml of water were successively poured into the mixture while stirring. The mixed gel was additionally stirred for 10 min at room temperature before crystallization. The composition of the gel mixture was $(TEA)_2O$: $0.0075NiO{:}0.30SiO_2{:}Al_2O_3{:}P_2O_5{:}10H_2O$. The mixed gel was transferred into a teflon vessel of 3.0 cm inner diameter and 10 cm height, it was then set in an autoclave of 300 ml. This was put into a dry oven set at 200°C, and kept for 8 h. The crystal formed was washed with distilled water by repeated cycles of centrifugation and decantation, followed by drying at 100°C for 12 h and calcination in air at 600°C for 3 h. The NiAPSO-34s prepared by the use of nickel nitrate and formate were designated as NiAPSO-34-N and NiAPSO-34-F, respectively. The prepared crystals were tabulated and crushed to 20–24 mesh to provide the reaction.

### 2.2. Adsorption of $H_2S$ or $SO_2$

In order to characterize the effect of sulfidation, adsorption of $SO_2$ or $H_2S$ was carried out as follows; in order to dehydrate the sample was preheated at a rate of 3°C/min for 30 min in a $N_2$ flow up to 500°C and kept for 30 min at that temperature. It was then exposed to $SO_2$ of 1.51 mol% or $H_2S$ of 2.04 mol% diluted with $N_2$ at 450°C for 2 h with a SV 1000 $h^{-1}$.

### 2.3. Characterization

Synthesized crystals were identified by powder X-ray diffraction analysis (XRD), by using Shimadzu XD-DI with Nickel filtered Cu $K\alpha$ radiation (30 kV, 30 mA) at an angle of $2\theta$ range from 50 to 5 degrees.

Composition of the crystals formed was analyzed by ICP-AES (inductively coupled plasma atomic emission spectrometry), Shimadzu ICPS-1000III.

Crystal sizes and morphology of the crystals were observed by using Hitachi S-2500CX scanning electron microscope (SEM).

UV–visible spectra were recorded on a Shimadzu MPS-2000 spectrometer, and $BaSO_4$ was used as the reflectance standard.

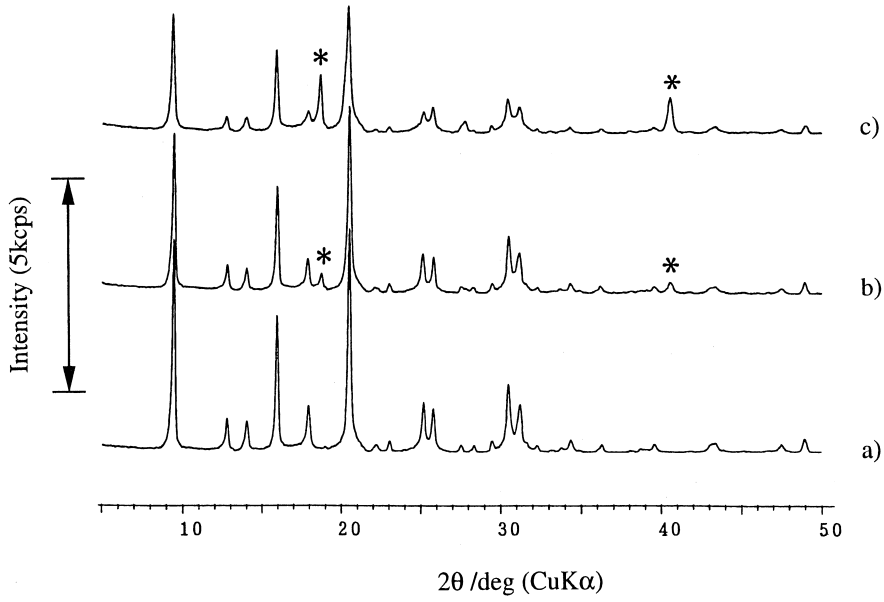


Fig. 1. XRD patterns for the crystals. (a) SAPO-34, (b) NiAPSO-34-N, (c) NiAPSO-34-F.

IR spectra were recorded on a Nicolet MAGNA-IR 560 spectrometer with Fourier transforms at room temperature by diffuse reflectance method. A 15 mg portion (Sample: KBr = 3:1) of fine crystals was packed in a ceramic cell with 5.0 mm inner diameter which was fixed with a high-temperature diffuse reflectance unit, it was treated at 450°C for 15 min in a 30 ml/min $N_2$ flows before the measurement. Fifty scans were accumulated under 4 $cm^{-1}$ resolution.

Acidity of the catalyst was estimated by TPD profiles for pre-adsorbed $NH_3$, determined by Quadruple Mass Spectrometer (M-QA100F) of BEL JAPAN To avoid an influence of water during the $NH_3$ adsorption, the adsorption was done at above 100°C.

### 2.4. Methanol conversion reaction

The methanol to hydrocarbon conversion was carried out by using an ordinary continuous flow apparatus. A 0.325 g portion (0.35 ml) of the catalyst was packed into a quartz tubular reactor having a 5.0 mm inner diameter, and a reaction gas composed of 15 mol% methanol and 1.51 mol% $SO_2$ or 2.04 mol% $H_2S$ diluted with $N_2$ was allowed to flow with a space velocity (SV) of 1000 $h^{-1}$ at a temperature range from 300 to 600°C, for 1–8 h on stream.

The reaction products were determined by three FID-type gas chromatographs and one TCD-type. The columns of VZ-10 for analysis of gaseous hydrocarbons, SILICON-OV-101 for analysis of gasoline range hydrocarbons, and

Table 1
Composition of the crystals

| Samples | Source of Ni | Solubility in 100 parts per water (r.t.) | ICP data (Al ≡ 1) | | |
|---|---|---|---|---|---|
| | | | Si | P | Ni |
| SAPO-34 | – | – | 0.250 | 0.750 | – |
| NiAPSO-34-N | Nitrate | 150 | 0.114 | 0.986 | 0.001 |
| NiAPSO-34-F | Formate | 2.56 | 0.072 | 0.786 | 0.083 |

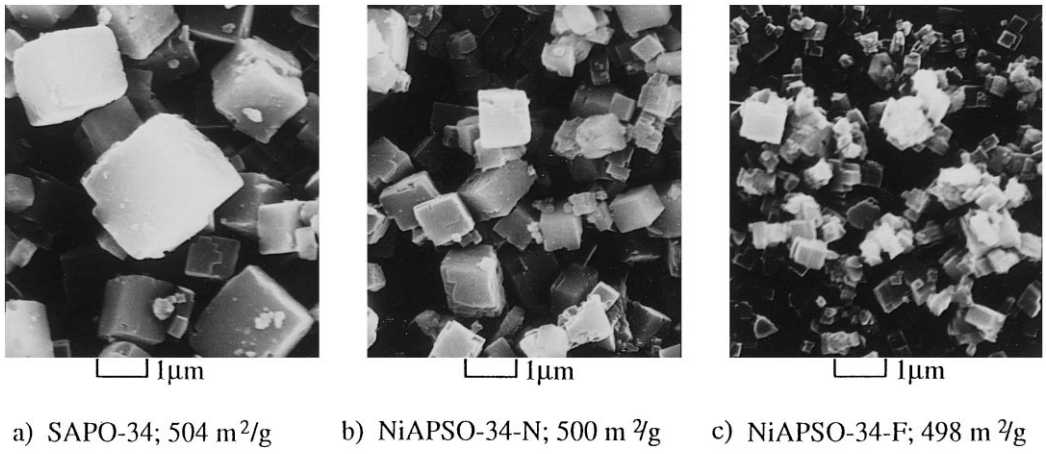


Fig. 2. SEM photographs and BET surface areas of samples.

Porapark T for analysis of methanol and dimethylether and activated carbon for CO and $CO_2$ were used.

## 3. Results and discussion

### *3.1. Physical properties of catalysts*

XRD patterns of NiAPSO-34 crystals were identified with US Patent literature [1] and are shown in Fig. 1. The peaks with asterisk are assigned to the nickel oxide. These peak intensities of NiAPSO-34-F were higher than those of NiAPSO-34-N, indicating that a considerable amount of non-incorporated nickel is occluded in crystal.

The composition of elements analyzed by ICP is shown in Table 1. The amount of nickel in the crystals prepared with nickel formate was 8 times as high as that with nickel nitrate.

Morphology of the crystals observed by SEM photograph is shown in Fig. 2 with their BET-surface areas. As shown in this figure, all samples were uniform cubic crystals of chabazite-like structure. The more the nickel content was, the smaller the crystal size. In particular, the size of NiAPSO-34-F was very small, and was less than a quarter of that of SAPO-34. The BET surface areas of calcined crystals possessed a wide area above 490 $m^2/g$ for all the crystal.

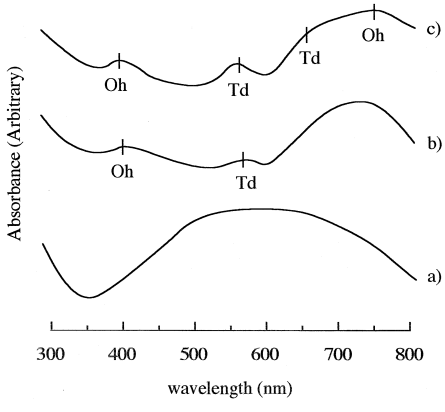


Fig. 3. UV–visible spectra of samples. (a) SAPO-34, (b) NiAPSO-34-N, (c) NiAPSO-34-F.

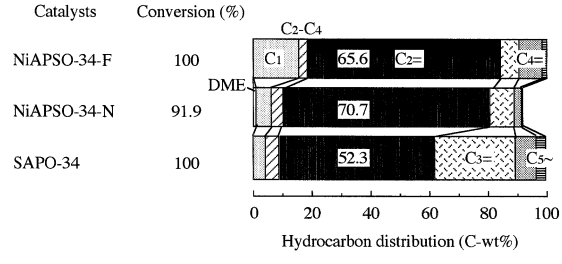


Fig. 4. Distribution of hydrocarbons produced on catalysts prepared from different nickel sources in methanol conversion. Reaction conditions: MeOH 15 mol%–$N_2$ 85 mol%; GHSV, 500 $h^{-1}$; Time on stream, 1 h; Temperature, 425°C.

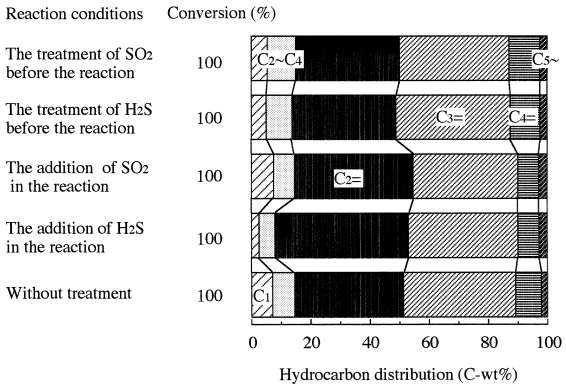


Fig. 5. Distribution of hydrocarbons produced on catalysts after 6 h on stream under different treatment conditions with sulfur compounds. Reaction conditions: MeOH 15 mol%; GHSV, 1000 $h^{-1}$; Time on stream, 6 h; Reaction temperature, 450°C.

In Fig. 3, UV–visible spectra are profiled. The coordination states of Ni observed by UV–visible measurement for NiAPSO-34-N and NiAPSO-34-F were octahedral, which appeared at both 400 and 750 nm [24], and tetrahedral spectra at 635 and 580 nm [25] indicating the incorporation of Ni into the framework of SAPO-34. The intensity of these bands for NiAPSO-34-F was stronger than that for NiAPSO-34-N. However, the tetrahedral-to-octahedral ratio could not be quantitatively determined.

### 3.2. Catalytic activity in methanol conversion

In Fig. 4, the catalytic activities of Ni-free SAPO-34, and NiAPSO-34-N and NiAPSO-34-F catalysts for methanol conversion are compared. As shown, the ethylene selectivity on Ni-incorporated SAPO-34 was increased compared with that of Ni-free SAPO-34. Furthermore, the methane yield on NiAPSO-34-F catalyst was higher than that on NiAPSO-34-N catalysts. This is ascribed to the higher concentration of non-incorporated nickel in NiAPSO-34-F.

In Fig. 5, distribution of hydrocarbons produced on methanol conversion after 6 h on stream under various reaction conditions are shown. Their conversions exhibited 100% under all conditions. The activity of the catalyst treated with $H_2S$ or $SO_2$ gas before the reaction was similar to that without treatment. The addition of $SO_2$ during the reaction did not affect the reaction. These indicate that sulfidation on nickel atom is not easy. However, addition of $H_2S$ gas in the reaction increased the ethylene selectivity and remarkably reduced methane yield.

More detailed data is summarized in Table 2, as shown, by the addition of $H_2S$, methanol conversion increased at most temperatures and

Table 2
Effect of reaction temperature on the catalytic performance under the conditions with and without $H_2S$ addition

| Conditions | Temperature (C°) | Conversion (%) | DME | Distribution of products (C-wt.%) | | | | | |
|---|---|---|---|---|---|---|---|---|---|
| | | | | $C_1$ | $C_2$–$C_4$ | $C_2=$ | $C_3=$ | $C_4=$ | $C_5$– |
| Without | 300 | 89.0 | 43.9 | 2.0 | 1.8 | 24.9 | 26.3 | 2.1 | 0.3 |
| treatment | 350 | 94.0 | 32.3 | 1.2 | 1.6 | 35.6 | 26.1 | 2.2 | 1.1 |
| | 400 | 97.0 | 16.3 | 2.3 | 3.5 | 46.6 | 27.0 | 2.7 | 1.7 |
| | 450 | 99.0 | 4.1 | 10.9 | 3.5 | 55.3 | 21.9 | 2.7 | 1.7 |
| | 500 | 100 | 0 | 50.5 | 3.4 | 37.1 | 7.2 | 1.0 | 0.9 |
| | 550 | 100 | 0 | 86.2 | 2.6 | 9.5 | 1.2 | 0.2 | 0.2 |
| | 600 | 100 | 0 | 93.0 | 1.8 | 4.9 | 0.4 | 0.2 | 0 |
| With the | 300 | 95.0 | 46.4 | 11.1 | 0 | 23.0 | 19.5 | 0 | 0 |
| addition | 350 | 96.0 | 0.4 | 2.9 | 5.5 | 50.0 | 34.8 | 5.5 | 1.8 |
| of $H_2S$ | 400 | 100 | 0 | 1.1 | 2.9 | 56.8 | 33.5 | 4.1 | 1.6 |
| | 450 | 100 | 0 | 2.9 | 4.9 | 44.1 | 38.0 | 6.9 | 3.3 |
| | 500 | 100 | 0 | 26.3 | 4.4 | 45.9 | 19.0 | 2.9 | 1.6 |
| | 550 | 100 | 0 | 64.8 | 3.5 | 25.4 | 4.9 | 0.8 | 0.6 |
| | 600 | 100 | 0 | 81.8 | 4.6 | 11.1 | 2.0 | 0.4 | 0.2 |

* Reaction conditions: GHSV, 1000 $h^{-1}$; time on stream, 1 h; methanol feed 15 mol%.

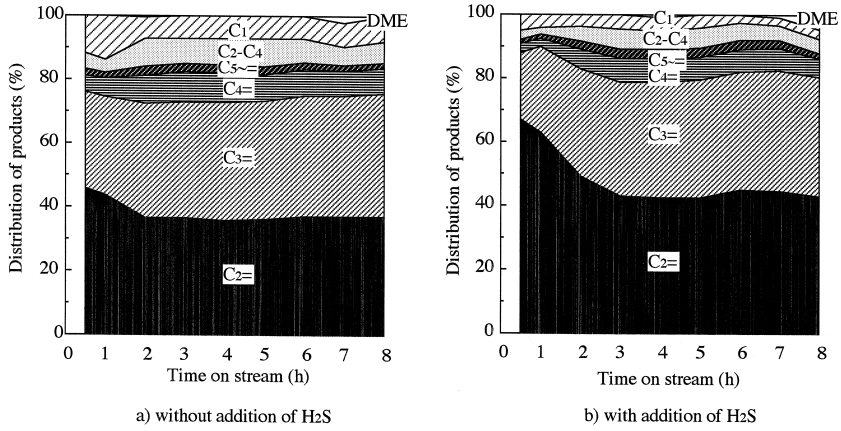


Fig. 6. Change in product distribution with an increase of time on stream under the conditions with and without $H_2S$ addition. Reaction conditions: MeOH 15 mol%; GHSV, 1000 $h^{-1}$; Time on stream, 8 h; Reaction temperature, 450°C.

methane yields remarkably decreased, which resulted in the increase of the ethylene selectivity. Since dimethyl ether formation was markedly decreased by the $H_2S$ addition, the acidity of the catalyst would be increased.

In Fig. 6, changes in the distribution of products with an increase of time on stream with and without $H_2S$ gas are shown. The $H_2S$ addition remarkably increased, decreased methane formation and increased ethylene formation.

From the results of Figs. 5 and 6, a model expected for adsorption of $H_2S$ could be supposed, as shown in Fig. 7. When $H_2S$ molecules were absorbed on NiAPSO-34 crystal, bands around 2100–2300 $cm^{-1}$ and 1500–1700 $cm^{-1}$ assigned to SH stretching and OH stretching, respectively, were observed from FR-IR. Consequently, it could be supposed that the $H_2S$ molecules are well absorbed on NiAPSO-34, and the $S^{2-}$ ions attack to the non-incorporated $Ni^{2+}$ ions to form nickel sulfide. Therefore, as a consequence, the methane yield generated on nickel oxide decreased in the methanol conversion.

### 3.3. Acidity

From the result of methanol conversion, it is suggested that increase of ethylene selectivity is ascribed to the increase of acidity in crystal by the addition of $H_2S$. The $NH_3$-TPD profiles for catalysts treated with and without $H_2S$ are shown in Fig. 8. These profiles consist of two peaks. One appears at a low temperature range around 150–180°C and another appears at a high temperature range around 420–470°C. The

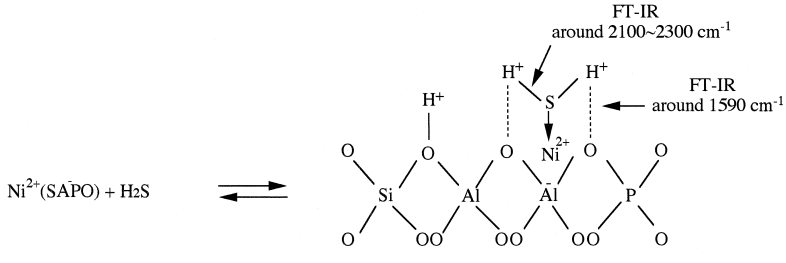


Fig. 7. A model supposed for adsorption of $H_2S$ on NiAPSO-34 crystals.

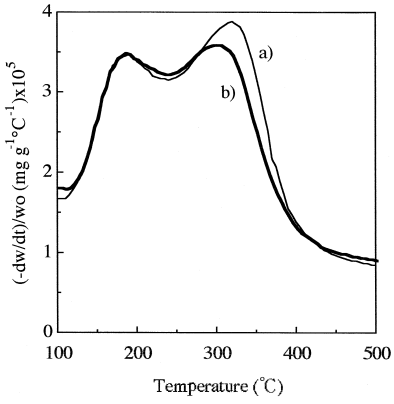


Fig. 8. $NH_3$-TPD profiles of samples with and without $H_2S$ treatment. (a) Without $H_2S$ treatment, (b) With $H_2S$ treatment.

low and high temperature peaks correspond to the weak and strong acid sites, respectively. It is a very surprising result that the acid sites at high temperature were somewhat reduced, whereas the weak acidity was not changed for the sample treated with $H_2S$ gas. This suppression that the ethylene produced is transferred to the higher hydrocarbon on strong acid sites. In conclusion, the ethylene selectivity on methanol conversion increased as nickel property was suppressed by sulfidation on NiAPSO-34-F.

## 4. Conclusions

The presence of $H_2S$ mainly contributed to the decrease in methanation activity caused on the Ni non-incorporated to the NiAPSO-34 framework, as the NiO changed to NiS. The reduction of the methanation activity brought about the increase in ethylene selectivity.

## Acknowledgements

This study was supported in part by Grant-in-Aid for Scientific Research on Priority Area 0724104 from the Ministry of Education, Science, Sports and Culture, Japan.

## References

[1] S.T. Wilson, B.M. Lok, E.M. Flenigen, US patent 4310440 (1982).
[2] J. Haggin, Chem. Eng. News, June 20 (1983) 36.
[3] T. Inui, H. Matsuda, H. Okaniwa, A. Miyamoto, Appl. Catal. 58 (1990) 155.
[4] T. Inui, S. Phatanasri, H. Matsuda, J. Chem. Soc., Chem. Commun. (1990) 205.
[5] J. Liang, H. Li, S. Zhao, W. Guo, R. Wang, M. Ling, Appl. Catal. 64 (1990) 31.
[6] J.M. Thomas, Y. Xu, C.R.A. Catlow, J.W. Coaves, Chem. Mater. 3 (1991) 667.
[7] T. Inui, Y. Takegami, Hydrocarbon Processing 61 (1982) 117.
[8] T. Inui, M. Kang, Appl. Catal. A: General 164 (1997) 211.
[9] M. Kang, T. Inui, 78th meeting of Catalysis Society of Japan, Abstract, 1996, p. 240.
[10] M. Kang, T. Inui, 80th meeting of Catalysis Society of Japan, Abstract, 1997, p. 300.
[11] M. Ziolek, J. Kujawa, O. Saur, A. Aboulayt, J.C. Lavalley, J. Mol. Catal., A: Chem. 97 (1995) 49.
[12] M. Guisnet, Stud. Surf. Sci. Catal. 20 (1985) 283.
[13] K. Tanabe, M. Misono, Y. Ono, H. Hattori, Stud. Surf. Sci. Catal. 51 (1989) 1.
[14] C. Lahousse, J. Bachelier, J.C. Lavalley, H. Lauron-Pernot, A.M. LeGovic, J. Mol. Catal. 87 (1994) 329.
[15] M. Waquif, A. Mohammed Saad, M. Bensitel, J. Bachelier, O. Saur, J.C. Lavalley, Chem. Soc. Farad. Trans. 88 (1992) 2931.
[16] R.M. Baldwin, S. Vinciguerra, Fuel 62 (1983) 498.
[17] H.G. Karge, M. Ziolek, M. Laniecki, Zeolites 7 (1987) 197.
[18] S. Hidaka, A. Iino, N. Goto, N. Ishikawa, T. Mibuchi, K. Nitta, Appl. Catal. 43 (1988) 57.
[19] M. Ziolek, I. Bresinska, Zeolites 5 (1985) 245.
[20] H.G. Karge, M. Ziolek, M. Laniecki, J. Catal. 109 (1988) 252.
[21] M. Sugioka, T. Nakyama, Y. Uemichi, T. Kanazuka, React. Kinet. Catal. Lett. 41 (1990) 345.
[22] M. Ziolek, K. Nowinska, K. Leksowska, Zeolites 12 (1992) 710.
[23] T. Inui, ACS Symp. Series, No. 398, Zeolite Synthesis, M.L. Occelli, H.E. Robson (Eds.), Amer. Chem. Soc., 1989, pp. 479.
[24] F.A. Cotton, G. Wilkinson, Advanced Inorganic Chemistry, 5th edn., Wiley, New York, 1988, p. 744.
[25] O. Schmitz-Dumont, H. Goessling, H.Z. Brokopf, Z. Anorg. Allgem. Chem. 300 (1959) 159.